Journal of Electronic Testing (2024) 40:107–116
https://doi.org/10.1007/s10836-024-06101-1

Research on the Reliability of Interconnected Solder Joints of Copper Pillars under Random Vibration

Shifeng Yu[1] · **Junjie Dai**[1] · **Junhui Li**[1]

Received: 25 October 2023 / Accepted: 16 January 2024 / Published online: 24 February 2024

Abstract
In this paper, the reliability of copper pillar micro-bump under random vibration is investigated. Three kinds of copper pillar solder joints with different morphologies were obtained by changing the hot press bonding process, and the random vibration fatigue simulation of flip-flop interconnect solder joints was carried out by using Ansys to obtain the stress–strain distribution law of the solder joints and predict the vibration fatigue life of the solder joints. It is found that the outermost solder joints of flip-flop bonding are most likely to fail; the fatigue life of copper pillar solder joints is predicted based on the three interval method, the Miner linear cumulative damage criterion and the high cycle fatigue formula; reliability experiments are conducted, and it is found that the drum solder joints are most prone to cracking, followed by hourglass and columnar shapes and that all cracks are caused by the substrate side of copper pillar. Cracks are sprouted from the contact surface between the copper pillar and solder on the substrate side and expand internally in the intermetallic compound (IMC) layer, while the presence of voids aggravates the generation of cracks.

Keywords Copper pillar bump · Flip chip · Random vibration · Vibration fatigue life

1 Introduction

With the development of three-dimensional integration technology, the application of electronic devices has become more and more extensive, and the environment in which it works has become diverse and harsh, such as in the automotive, aerospace, medical and other industries, to improve the effectiveness of the package, which poses a new challenge to the reliability of microelectronic packaging [1, 17, 20]. In some cases, vibration can be a major factor in the failure of electronic devices [21]. Under the action of vibration, the electronic components will undergo dynamic bending deformation, thus the solder joints between the substrate and the chip are subjected to repeated stress–strain, causing elastic and plastic deformation of the solder joints, which ultimately leads to the formation of cracks. A crack will increase the electrical resistance at the bonding interface until a break occurs and the device will become non-functional. The failure of solder joints subjected to shock and vibration is the main failure mechanism in electronic products, and the vibration reliability of solder joints has always been a concern in the microelectronics industry [15].

Vibration reliability of solder joints has already been investigated by many researchers. Steinberg [19] presented extensive research and methodology on the analysis and reliability of electronic equipment under vibration and drop/shock loads. Wong et al. [22] explained the failure to be due to the simultaneous axial and shear deformation and coupling moments experienced at the solder interconnections. Due to the development of auto-driving cars, vibration reliability is getting more and more attention, and there are many researches on the development of new methods and techniques. Yu et al. [24] developed an evaluation method based on vibration testing and finite element analysis (FEA) for predicting the fatigue life of

Responsible Editor: V. D. Agrawal.

✉ Junhui Li
lijunhui@csu.edu.cn

Shifeng Yu
ysf572595801@163.com

Junjie Dai
djj19970210@163.com

[1] State Key Laboratory of Precision Manufacturing for Extreme Service Performance Manufacturing and School of Mechanical and Electrical Engineering, Central South University, Changsha 410083, China

electronic components under random vibration, showing good fatigue life prediction. Xie et al. [23]. proposed a new method for vibration testing of automobiles and consumer electronic devices through sine-sweeping and random vibration experiments in combination with finite element analysis, and Khaldarov et al. [7, 8]. proposed a simplified method for analyzing random vibration for calculating vibration in solder joints experiencing high and ultra-high cycle fatigue, and also analyzed the failure mechanisms of copper traces and solder joints. Gharaibeh et al. [4, 5] demonstrated that it is possible to calibrate finite element modal vibration models by correlating the simulated vibration properties with experimental results as well as measured printed circuit board (PCB) strains. Sushil Doranga et al. [2, 3] used sine sweep and stepped sine testing to obtain the maximum vibration amplitude of the samples, correlated the experimental results with a finite element model, and also developed a global–local finite element model to analyze the fatigue of the solder joints. The microscopic mechanism of solder joint failure under random vibration is also a focus of attention. For example, Liu et al. [16] experimented and analyzed high cycle vibration fatigue in ball grid array (BGA) packages. Their experimental system provided controls for varying the cyclic frequency and the amplitude of the applied load. Direct visual inspection was used to record the failure of solder joints. It was observed that BGA interconnect failures were due to cracks sprouting and expanding along the nickel/tin solder interface between the BGA solder balls and the electroless nickel/immersion gold plating on the plastic ball grid array (PBGA) substrate copper sheet. Liu et al. [15] conducted vibration reliability experiments on lead-free BGA solder joints and found that with the increase of random vibration intensity, the damage location of the solder joints changes and the damage form of the solder joints changes from fatigue cracks to brittle cracks, and it was also found that the damage mechanism of the solder joints under large power spectral density (PSD) acceleration amplitude is similar to that under impact loading. Majid et al. [18] found that the solder joints in BGA packages are subjected to the highest peeling stresses, which are concentrated at the interface between the solder joints and the PCB, and it was also found that the devices furthest away from the BGAs have the longest fatigue life [13]. In terms of improving vibration fatigue life, Libot et al. [14] found that SAC305 has a higher vibration fatigue life than Sn62Pb36Ag2 at 20 °C, and the vibration fatigue life of solder joints is lower at low temperatures due to low-temperature brittleness, and suggested that the solder joint shape may have an effect on the fatigue life as well. Lall et al. [10] investigated the vibration fatigue life of SAC105 and SAC305 the vibration fatigue life of solder joints at different temperatures was found to decrease significantly with increasing temperature. Gharaibeh et al.. [6] found that the smaller size and thicker thickness of PCBs, and the larger size and thicker thickness of integrated circuits can improve the fatigue life, in relevant experimental demonstrations and theoretical modelling, stiffened PCB have been shown to have more than three times the life of solder balls. because even though the amplitude of the acceleration increases, the relative motion between the PCB and the package decreases [2].

At present, there are fewer research reports on the random vibration fatigue reliability of copper pillar bumps, and the influence and mechanism of the shape of the solder joints on their vibration reliability are still unclear. In this paper, Ansys was used to analyze the stress–strain distribution of the welded joints under random vibration, and to determine the location of the solder joints that are most vulnerable to failure in flip-flop bonding; experiments were conducted on three different shapes of solder joints obtained by changing the bonding process to predict the vibration fatigue life of copper pillar solder joints based on the three-interval method. Finally, reliability experiments were conducted to study the failure mechanism of the solder joints.

2 Method and Experiment

2.1 Sample Production

The daisy chain diagram of the chip and substrate used in this paper is shown in Fig. 1. Each sample contains two symmetrical daisy chains, and each daisy chain contains 28 copper pillars. The chip size is 6×6×0.5 mm with a copper pillar height of 15 μm, the substrate size is 12×12×0.8 mm with a copper pillar height of 30 μm, and the copper pillar diameters are both 100 μm. The solder caps of the chip copper pillars are made of Sn3.5Ag with a thickness of about 25 μm. The assembly is performed by thermal compression bonding (TCB), the thermal compression bonding parameters shown in Fig. 2, and the main parameters of TCB include bonding pressure, chip temperature, holding time

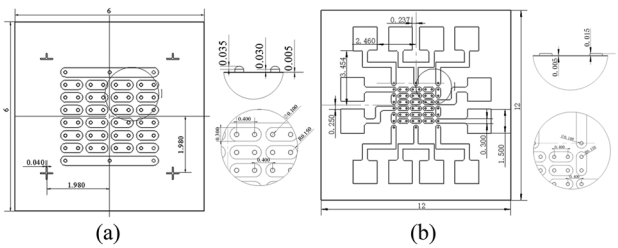

Fig. 1 Flip Chip Diagram **a** chip solder joint array **b** substrate copper pillar array

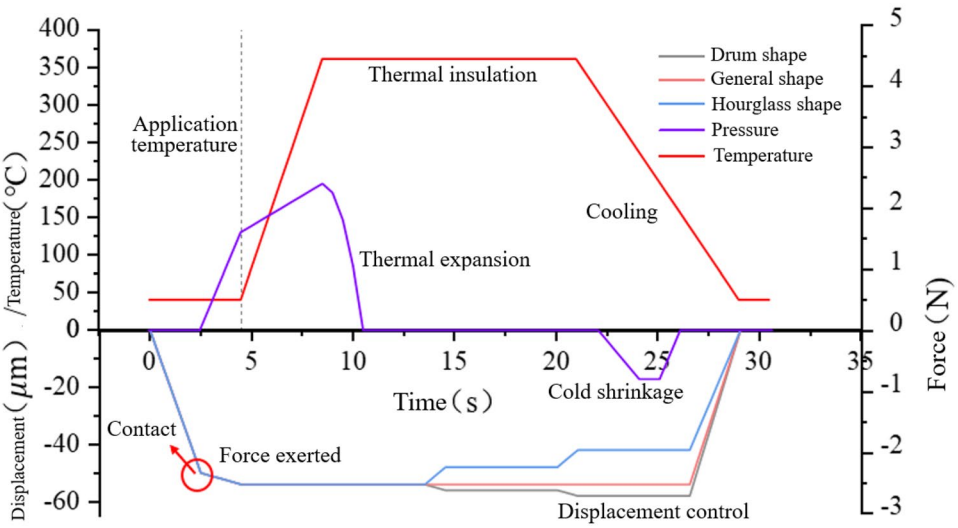

Fig. 2 Hot pressing process curve

and lifting height, and the three morphologies obtained are shown in Fig. 3. Test vehicle shown in Fig. 4 consisted of a PCB, substrate, chip, and solder balls.

2.2 Finite Element Analysis

To study the stress–strain distribution of the solder joints under the action of random vibration, finite element software is used to carry out random vibration simulation on the flip chip and PCB, and the overall finite element model of the random vibration device is shown in Fig. 5. In this paper, to simplify the model and save calculation time, the simulation model only has a flip chip. There are 281050 meshes and 1387432 nodes in total. The PCB is constrained by four positioning holes around it. The material used for the chip is Si. The solder joint material is Sn3.5Ag. Substrate and PCB materials are FR-4. The specific properties parameters of each material are shown in Table 1. The parameters are taken from the room temperature. All the material properties are linear elastic models, and all materials are considered isotropic.

The modal analysis is first performed through the Modal module of Ansys software. Then in the Random Vibration module in Ansys, the PSD function is added to apply random vibration load to the flip chip, and the PSD load is added at the four positioning holes of the constraints with the direction perpendicular to the chip. The minimum frequency of the random vibration is 50 Hz, the maximum frequency is 2000 Hz, the maximum power spectral density is $0.3G^2/Hz$, the total root-mean-square (RMS) value of the acceleration is 207.1 m/s^2, and the gravitational acceleration is 9.8 m/s^2. Specific PSD is shown in Fig. 6.

The fatigue life of the copper pillar solder joints was predicted using the three-interval method, the linear cumulation damage criterion, and the high cycle fatigue formula. The three-interval method is a method proposed by Steinberg [19] by collating and rearranging a large amount of experimental data. The three-interval method assumes that the instantaneous acceleration or strain at a point on the device during a random load to which the device is subjected is a time-dependent random process, and that this process obeys a normal distribution. The three-interval method is shown in Eqs. (1)–(5):

$$n_1 = N_0^+ T_s(3600sec/hr)(0.6831) \tag{1}$$

$$n_2 = N_0^+ T_s(3600sec/hr)(0.271) \tag{2}$$

$$n_3 = N_0^+ T_s(3600sec/hr)(0.0433) \tag{3}$$

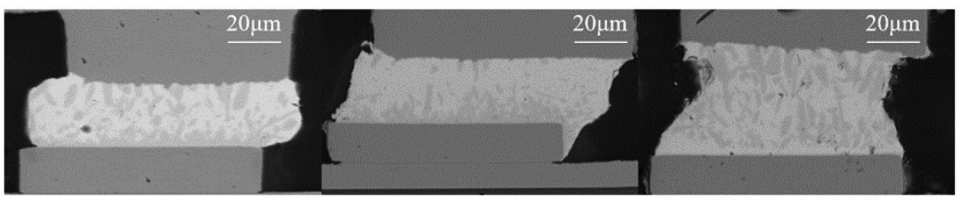

Fig. 3 Three different morphological samples

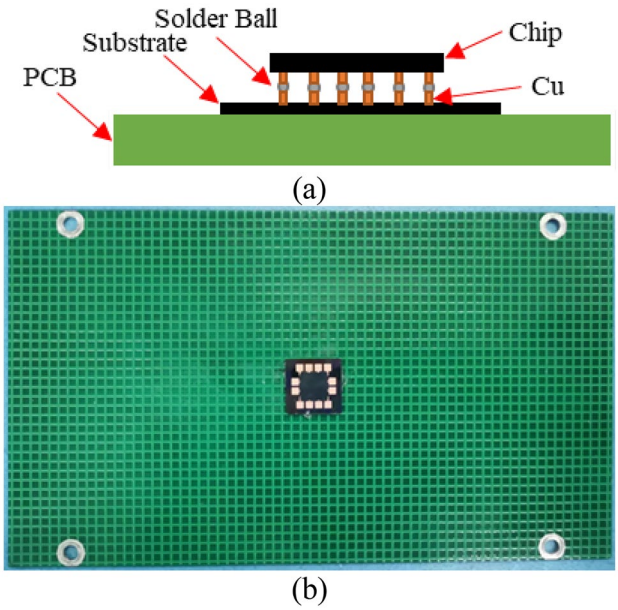

Fig. 4 Test vehicle **a** schematic diagram of z-axis direction, **b** actual picture

$$N_0^+ = \frac{1}{2\pi}\left[\frac{\frac{\pi}{2}P_1 f_1 Q_1}{\Omega_i^2} + \frac{\frac{\pi}{2}P_2 f_2 Q_2}{\Omega_2^2} + \cdots}{\frac{\pi}{2}P_1 f_1 Q_1}{\Omega_i^4} + \frac{\frac{\pi}{2}P_2 f_2 Q_2}{\Omega_2^4} + \cdots\right]^{\frac{1}{2}} \tag{4}$$

$$Q_i = \sqrt{f_i} \tag{5}$$

For a mildly damper system with multiple peaks, each peak can be analogized to a system with a single degree of freedom to obtain Eq. (4), and according to a study by Hongfang Wang of Shanghai Jiao Tong University, the transfer rate of each peak can be calculated based on Eq. (5). In Eqs. (1)–(4), n_i is the cumulative number of cycles under $i\sigma$ strain level ($i=1,2,3$), T_s is the random vibration time, $N_0{}^+$ is the average number of passes through the axes with a positive slope per unit time in a graph with time as the horizontal axis and acceleration or strain as the vertical axis, P is the power spectral density at peak frequency, f_i is the first ($i=1,2,3$) natural frequency of a PCB assembly, Q is the transmittance, Ω is the angular frequency.

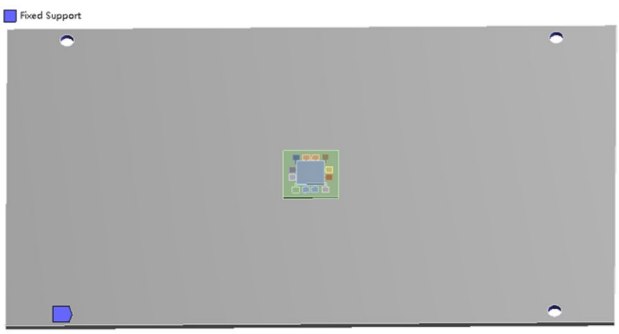

Fig. 5 Random vibration modeling and constraint

Table 1 Basic material properties [9, 12]

Material	Cu	Sn3.5Ag	Si	FR-4
Poisson's ratio	0.34	0.35	0.28	0.39(XZ&YZ 0.11(XY)
Density (kg/m3)	8960	6540	2329	1910
modulus of elasticity (GPa)	130	30.52	170	26.37(X,Y)11.8(Z)

The Miner linear cumulative damage criterion:

$$D_v = \frac{n_1}{N_1} + \frac{n_2}{N_2} + \frac{n_3}{N_3} \tag{6}$$

where D_v is the fatigue damage factor, often taken as 0.7, N_i is the number of fatigue cycles under $i\sigma$.

The high cycle fatigue formula:

$$\varepsilon_i = 3.5\frac{\sigma_u}{2E}N_i^{-0.12} \tag{7}$$

where ε_i is the maximum equivalent elastic strain at $i\sigma$, σ_u is the tensile strength of the material, the tensile strength of the solder joint material Sn3.5Ag is taken as 25 MPa at room temperature [11] and E is the modulus of elasticity of the material.

The equivalent strain amplitude in the strain singularity region of the solder joint is averaged through Eqs. (8) and (9):

$$\varepsilon = \frac{\sum \varepsilon_i V_i}{\sum V_i} \tag{8}$$

$$\varepsilon = \sqrt[\frac{\sqrt{2}}{3}]{\left(\varepsilon_x - \varepsilon_y\right)^2 + \left(\varepsilon_y - \varepsilon_z\right)^2 + \left(\varepsilon_z - \varepsilon_x\right)^2} + \frac{3}{2}\left(\gamma_{xy^2} + \gamma_{yz^2} + \gamma_{zx^2}\right) \tag{9}$$

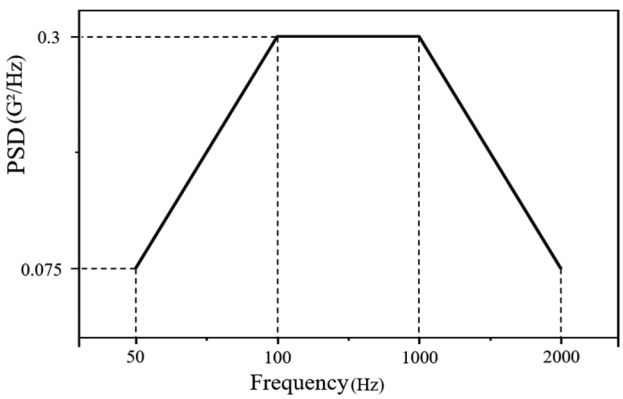

Fig. 6 PSD curves for random vibration simulation

Table 2 Random vibration test curve power spectral density

Test frequency (Hz)	PSD ($(m/s^2)^2/Hz$)
50	7.5
100	30
1000	30
2000	7.5

Equation (8) where ε is the equivalent strain amplitude, ε_i is the strain amplitude of a single mesh, and V_i is the mesh volume. In Eq. (9) $\varepsilon_i(i = x, y, z)$, and $\gamma_{ij}(i, j = x, y, y \text{and} i \neq j)$ are the positive and shear strains within each mesh.

2.3 Test Conditions and Analysis

The random vibration test was performed using an electrodynamic shaker with the test conditions shown in Table 2, the acceleration RMS value is 20.71 g. After the random vibration test, the sample will be sealed with epoxy resin, and grinding samples with 80, 240, 800, 1500 purpose sandpaper. The samples were polished with 0.5 µm diamond polishing solution. Then the microstructure was observed by scanning electron microscopy (SEM). Finally, the composition of the interfacial reaction products was analyzed using energy dispersive X-ray (EDX) analysis.

3 Results and Discussion

3.1 Stress and Strain Distribution and Fatigue Life Analysis During Random Vibration

The first 12 orders of natural frequency of modal analysis are shown in Table 3, since the highest frequency used for the random vibration experiment is 2000 Hz, the modal frequency viewed is $1.5f_{max} = 3000Hz$.

Table 3 First twelfth order modal analysis of copper pillar interconnection solder joints on the PCB

Ordinal number	Natural frequency (Hz)
1	428.75
2	775.83
3	1032
4	1179.1
5	1485.2
6	1762.2
7	1843.1
8	2465
9	2737.7
10	2899.8
11	3242
12	3410.1

Figures 7 and 8 show the 1σ stress–strain distribution of the flip-flop copper pillar solder joints, and it can be seen that the chip under random vibration is subjected to the outermost solder joints with the largest statistical value of stress–strain, which is due to the constraints on the four corners of the PCB, resulting in the deformation of the PCB in the random vibration, and in this deformation, the center of the chip's solder joints do not vary much with respect to the PCB's position, and the surrounding solder joints vary more with regard to the PCB's position, and so the outermost chip's solder joints have a large stress–strain under random vibration. The enlarged view of the solder joint shows that the maximum stress–strain of the solder joint occurs on the side close to the PCB, and the stress–strain in the middle of the solder joint is relatively small, so that the crack of the solder joint occurs at this position at the very beginning, and the maximum value of the 1σ stress is 3.4889MPa and the value of the strain in the direction of the Z-axis under the 1σ is 0.00016931mm/mm. In general, the first failure location in the chip under random vibration is the outermost solder joints, and the first crack is on the side of the copper pillar solder joints near the PCB.

In this paper, the three-interval method is used to predict the random vibration fatigue life of the copper pillar flip-flop solder joints, and the equivalent strain of the solder joints from $1\sigma \sim 3\sigma$ is obtained through simulation. The vibration fatigue life of the copper pillar solder joints can be obtained as 281 h through the calculation of Eqs. (1)–(9).

3.2 Influence of Solder Joint Structure on the Vibration Fatigue Life of Solder Joints

3.2.1 Effect of Solder Joint Height on Fatigue Life of Flip Chip

First, the volume of the solder joint is fixed at 1.845E-4mm3, the copper column diameter is 0.1 mm, and the height of the solder joint varies from 0.0185 mm to 0.032 mm. Table 4 shows the results obtained according to the three-interval method.

Figure 9 shows the relationship between the vibration fatigue life of the solder joint and the height of the solder joint, When the height of the solder joint is 0.02 mm, the vibration fatigue life is maximum 356.58 h. When it is less than this height, the vibration fatigue life increases with the increase of the height, and when it is higher than this height, the vibration fatigue life also decreases with the increase of the solder joint. when the height is 0.02 mm, the fatigue life is more than two times of other heights.

Figure 10 shows the strain distribution of different solder joint heights, from the figure can be found with the

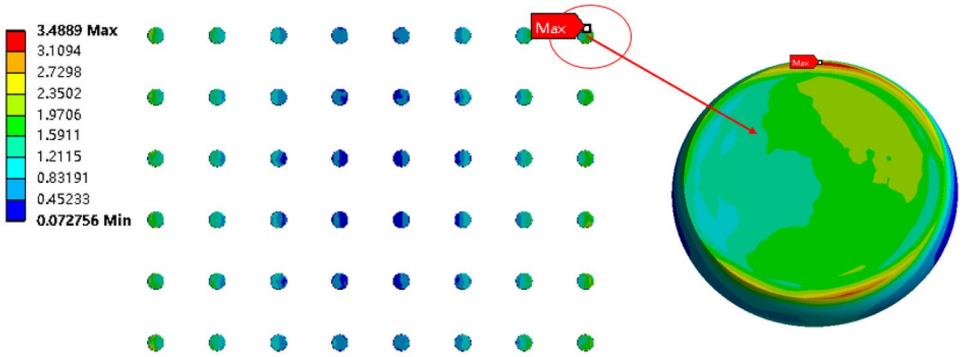

Fig. 7 Cloud view of 1σ stress distribution in flip-flop solder joints

increase in the height of the solder joint, the location of the maximum equivalent elastic strain from the bottom of the solder joint gradually shifted to the middle of the solder joint, which may lead to inconsistency in the location of the random vibration solder joint failure, that is, hourglass-shaped solder joints vulnerable to failure in the middle of the solder joint. The maximum strain of the solder joint is shifted to the middle of the solder joint probably because the deformation of the PCB under random vibration will pull on the solder joint, and when the PCB bends upward, it will stretch the solder joint, and because the hourglass-type solder joint is relatively thin in the neck, the stress strain here is larger, and it becomes a failure-prone solder joint.

3.2.2 Effect of Solder Joint Volume on Fatigue Life of Flip Chip

The fixed solder joint height is 0.023 μm, the copper pillar diameter is 0.1 mm, and the solder joint volume varies from 1.454E-4mm3 to 2.292E-4mm3. Table. 5 shows the results obtained according to the three-interval method.

Figure 11 shows the relationship between the fatigue life of the solder joint and the volume of the solder joint, the vibration fatigue life of the solder joints increases and then decreases as the volume of the solder joints increases. When the volume of the solder joint is 2.103E-4mm3, the vibration fatigue life is maximum 280.97 h; when the volume of the solder joint is 1.454E-4mm3, the vibration fatigue life is minimum 18.64 h. Therefore, increasing the volume of the solder joint can improve the resistance of the solder joint to vibration to some extent.

3.2.3 Effect of Copper Pillar Diameter on Fatigue Life of Flip Chip

The fixed solder joint volume is 1.845E-4mm3, the solder joint height is 0.023 mm, and the copper pillar diameter varies from 0.09–0.11 mm, Table 6 shows the results obtained according to the three-interval method.

Figure 12 shows the relationship between the fatigue life of the solder joint and the diameter of the copper pillar, with the increase of the diameter of the copper pillar, the vibration fatigue life of the solder joint has no obvious law. When the diameter of the solder joint is 0.1 mm, the maximum vibration fatigue life of the solder joint is 182.57 h, and when the diameter of the copper pillar is 0.11 mm, the minimum vibration fatigue life of the solder joint is 32.98 h.

3.3 Reliability Test of Different Structure Solder Joints

Figure 13 shows the solder joint images of the three shapes of solder joints at random vibration for 4 h, from which neither the column shape nor the hourglass shape produces obvious cracks, whereas the drum shape solder joint can be seen in Fig. 15f that there is already a slight crack produced, the cracks are located at the IMC where the copper pillar on

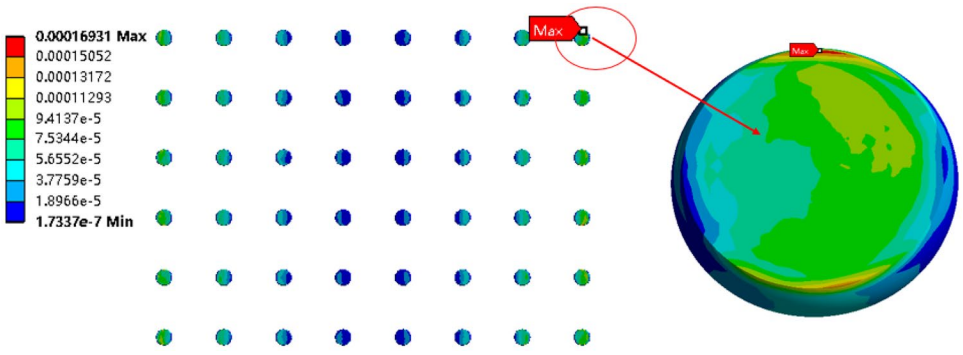

Fig. 8 Cloud view of 1σ strain distribution in flip-flop solder joints

Table 4 Relationship between solder joint height variation and vibration fatigue life

Number	1	2	3	4	5
Pad Diameter(mm)	0.1	0.1	0.1	0.1	0.1
Solder Joint volume(mm^3)	1.845E-4	1.845E-4	1.845E-4	1.845E-4	1.845E-4
Solder Joint height(mm)	0.0185	0.02	0.023	0.028	0.032
D_v	0.0143	1.96E-3	3.38 E-3	9.67 E-3	0.0139
Vibration fatigue life(h)	48.93	356.57	182.57	72.38	50.19

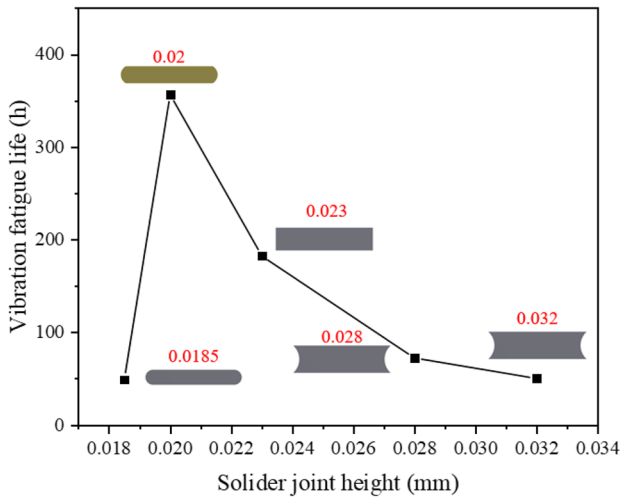

Fig. 9 Fatigue life of a solder joint as a function of solder joint height

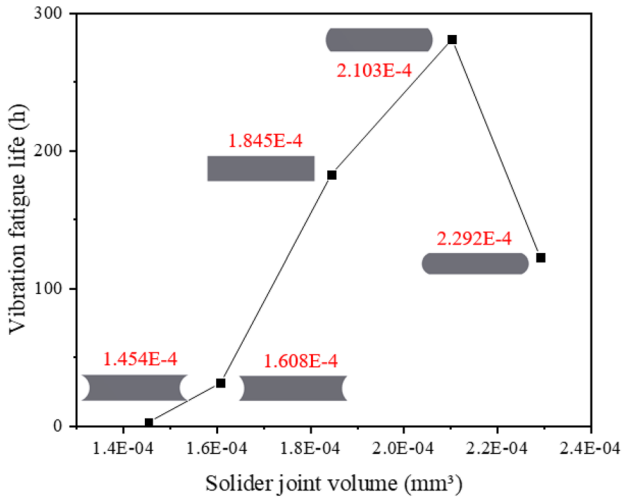

Fig. 11 Fatigue life of a solder joint as a function of solder joint volume

Fig. 10 Strain distribution at different solder joint heights: **a** 0.0185 mm; **b** 0.023 mm; **c** 0.032 mm

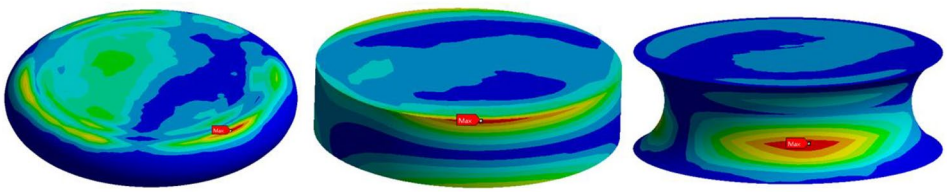

Table 5 Relationship between solder joint volume variation and vibration fatigue life

Number	1	2	3	4	5
Pad Diameter(mm)	0.1	0.1	0.1	0.1	0.1
Solder Joint volume(mm3)	1.454E-4	1.608E-4	1.845E-4	2.103E-4	2.292 E-4
Solder Joint height(mm)	0.023	0.023	0.023	0.023	0.023
$D_v(h^{-1})$	0.0376	0.0226	3.83E-3	2.49E-3	5.73E-3
Vibration fatigue life(h)	18.64	31	182.57	280.97	122.0 5

Table 6 Relationship between copper pillar diameter variation and vibration fatigue life

Number	1	2	3	4	5
Pad Diameter(mm)	0.09	0.095	0.1	0.105	0.11
Solder Joint volume(mm3)	1.845E-4	1.845E-4	1.845E-4	1.845E-4	1.845E-4
Solder Joint height(mm)	0.023	0.023	0.023	0.023	0.023
D_v	5.26E-3	0.0102	3.83E-3	6.91E-3	0.0212
Vibration fatigue life(h)	133.15	68.67	182.57	113	32.98

the substrate side contacts the solder. The chip side solder joints did not produce obvious cracks.

Figure 14 shows the solder joints after 8 h of random vibration, from the figure it can be found that the three kinds of shape of the solder joints have different degrees of cracks, and cracks are generated from the substrate side of the copper pillar in the contact surface of the solder, the chip side is still no cracks, and at the same time from the finite element analysis, the maximum stress and strain of the solder joints appeared in the substrate side of the copper pillar in the contact surface of the solder. The location of crack growth in random vibration verifies the reliability of the simulation. Comparing Fig. 13d with Fig. 14d, it is found that the cracks in the solder joint suddenly increase a lot with 4 h more random vibration because the solder joint in Fig. 14d are filled with IMC and the copper pillar on the side of the substrate have micro holes, so longer cracks are produced during random vibration.

Figure 15a shows the diagram of some solder joints with bad bonding quality, from which it can be found that when there is a hole on the side of the solder joint and the copper pillar of the substrate, cracks are very easy to be generated during the vibration process, especially in the place where IMC is abundant, Fig. 15b shows the graph of IMC less hourglass shaped solder joint, which is found to have almost no crack generation in the presence of a hole as compared to Fig. 14d, probably due to the absence of IMC at the place where this hole is generated, thus IMC has a great impact on the random vibration reliability of the solder joint and its generation should be avoided as much as possible.

From the above analysis, the cracks of the three different solder joints started to grow at the contact surface between the copper pillar and the solder on the side of the substrate, and the first to crack is the drum joint followed by the hourglass and pillar joints. In the process of random vibration, the PCB board will fluctuate up and down with the vibration will produce tensile and compressive stress and strain on the solder joints, in this kind of alternating stress, the solder joints will produce internal damage, when the damage accumulates to a certain degree, cracks will be produced. On the other hand, during the flip bonding process, IMC is generated inside the solder joint, and the nature of IMC with low temperature brittleness does not match the nature of the solder, resulting in stress concentration at the interface.

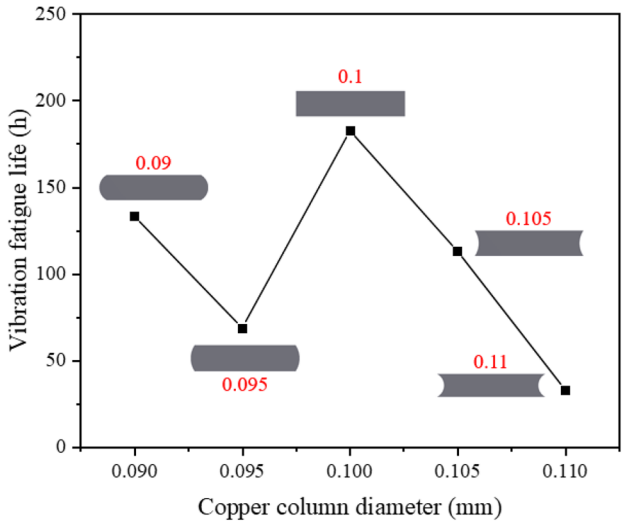

Fig. 12 Fatigue life of solder joints as a function of copper pillar diameter

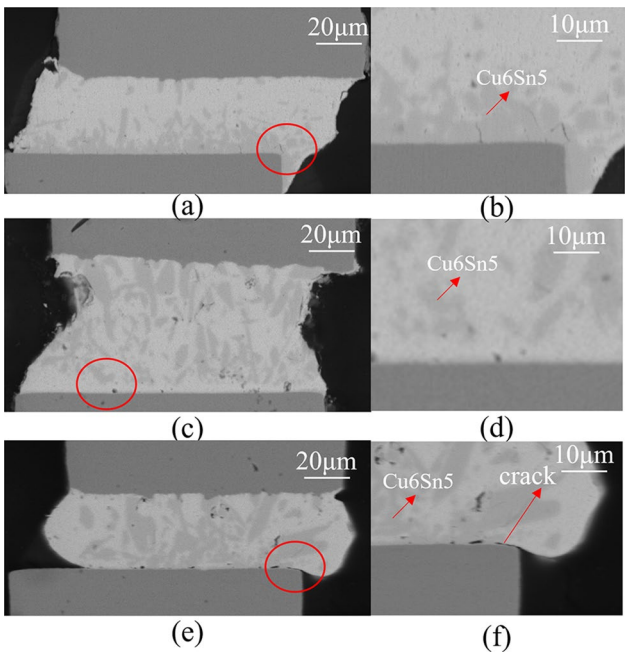

Fig.13 SEM image of solder joints with 4 h random vibration **a** column overall; **b** column partial; **c** hourglass overall; **d** hourglass partial; **e** drum overall; **f** drum partial

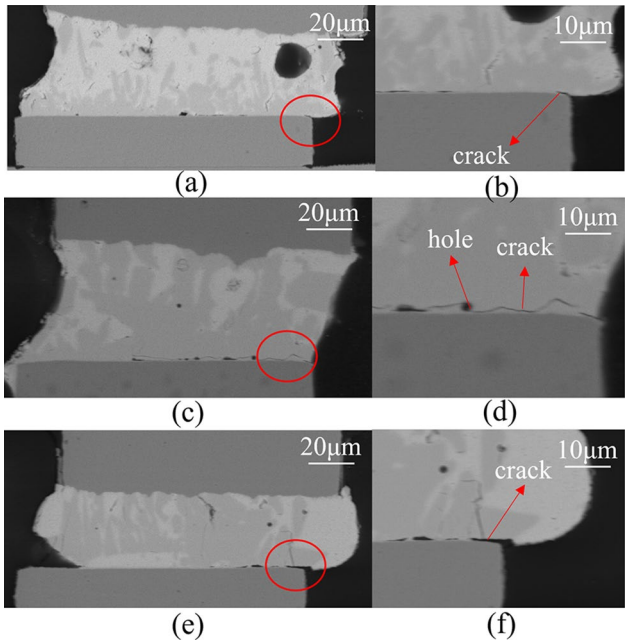

Fig.14 SEM image of solder joints with 8 h random vibration **a** column overall; **b** column partial; **c** hourglass overall; **d** hourglass partial; **e** drum overall; **f** drum partial

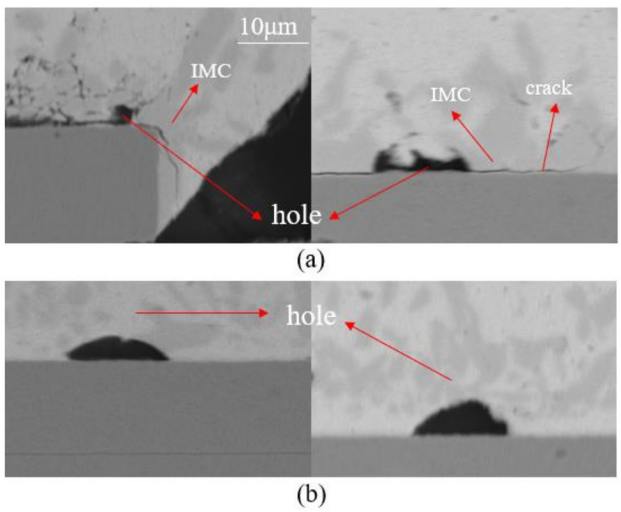

Fig.15 SEM image of solder joints with poor bonding quality **a** with voids and cracks; **b** with voids and no cracks

Under these two factors, the solder joint cracks at the IMC layer and expands until it fails.

4 Conclusion

(1) In the random vibration process is in the outermost layer of the flip chip solder joints subject to the greatest stress strain, is the weakest solder joints in the entire chip (prone to failure).

(2) Control the volume of the solder joint and copper pillar diameter is constant, when the height of the solder joint has 0.0185 mm-0.032 mm change, the fatigue life of the solder joint is maximum when the height of the joint is 0.02 mm, and as the height of the joint increases, the failure position of the joint gradually moves to the middle of the joint; control the height of the solder joint and copper pillar diameter is constant, when the volume of the solder joint from 1.454E-4mm3-2.292E-4mm3 change, fatigue life of solder joints increases and then decreases; controlling the volume of the solder joint and the height of the solder joint constant, when the diameter of the copper column changes from 0.09 mm-0.11 mm, there is no clear pattern in the fatigue life of solder joints.

(3) Under the effect of random vibration, the cracks of solder joints are located at the IMC of the contact surface between the copper pillar and the solder joints on the side of the substrate, and the solder joints with the first cracks are located at the periphery of the chip and are very prone to cracks when there are holes in the IMC layer. For all three shapes, the drum shape is the most prone to cracking, followed by the hourglass and column shapes.

Funding This work was supported by National Natural Science Foundation of China joint fund for regional innovation and development (No. U20A6004).

Data Availability The datasets generated during and/or analyzed during the current study are available from the corresponding author on reasonable request.

References

1. C¸ELİK, M. and GENC¸, C. (2008) Mechanical fatigue of an electronic component under random vibration. Fatigue Fract Eng Mater Struct 31:505–516
2. Doranga S, Schuldt M, Khanal M (2022) Effect of Stiffening the Printed Circuit Board in the Fatigue Life of the Solder Joint. Materials 15:6208
3. Doranga S, Xie D, Lee J, Zhang A, Shi X, Khaldarov V (2023) A Time Frequency Domain Based Approach for Ball Grid Array Solder Joint Fatigue Analysis Using Global Local Modeling Technique. ASME J Electron Packag 145(3)
4. Gharaibeh MA, Su QT, Pitarresi JM, Anselm M (2013) Board-Level Drop Test: Comparison of Two ANSYS Modeling Approaches and Correlation with Testing[C]. Adv Res Electron Assy (AREA) Consortium
5. Gharaibeh MA, Su QT, Pitarresi JM, Anselm M (2013) Modeling and Characterization for Vibration [C]. Adv Res Electron Assy (AREA) Consortium
6. Gharaibeh MA, Pitarresi JM (2019) Random vibration fatigue life analysis of electronic packages by analytical solutions and Taguchi method [J]. Microelectron Reliab 102
7. Khaldarov V, Zhang A, Xie D, Lee J, Shi X, Roucou R, Doranga S, Jian M, Kelly B, Shalumov A (2023) New Methodology

Assessment of Copper Trace and Solder Joint Fatigue Failures in Board-level Random Vibrations for Automotive Applications. IEEE 73rd Electron Compon Technol Conf (ECTC) Orlando FL, USA 412–419
8. Khaldarov V, Zhang A, Xie D, Lee J, Shi X, Roucou R, Doranga S, Shalumov A (2022) Solder Joint Fatigue Studies Subjected to Board-level Random Vibration for Automotive Applications. IEEE 72nd Electron Compon Technol Conf (ECTC). San Diego, CA, USA 1777–1784
9. Lall P, Islam MN, Singh N, Suhling JC, Darveaux R (2004) Model for BGA and CSP reliability in automotive underhood applications. IEEE Trans Compon Packag Technol 27(3):585–593
10. Lall P, Yadav V, Locker D (2020) Sustained High-Temperature Vibration Reliability of Thermally Aged Leadfree Assemblies in Automotive Environments [C]. 2020 Pan Pacific Microelectron Symp (Pan Pacific)
11. Lang F, Tanaka H, Munegata O, Taguchi T, Narita T (2005) The effect of strain rate and temperature on the tensile properties of Sn–3.5Ag solder. Mater Charac 54(3):223–229 (ISSN 1044–5803)
12. Lau JH, Lee S (2002) Modeling and analysis of 96.5Sn-3.5Ag lead-free solder joints of wafer level chip scale package on buildup microvia printed circuit board [J]. Electron Packag Manuf IEEE Trans 25(1):51–58
13. Leslie D, Heid T, Dasgupta A (2018) Effect of temperature on vibration fatigue of SAC105 solder material after extended room temperature aging [C]. 1–5
14. Libot JB, Arnaud L, Dalverny O, Alexis J, Milesi P, Dulondel F (2016) Mechanical fatigue assessment of SAC305 solder joints under harmonic and random vibrations. 2016 17th International Conference on Thermal, Mechanical and Multi-Physics Simulation and Experiments in Microelectronics and Microsystems (EuroSimE), Montpellier, France. 1–8
15. Liu F, Meng G (2014) Random vibration reliability of BGA lead-free solder joint. Microelectron Reliab 54(1):226–232 (ISSN 0026–2714)
16. Liu X, Sooklal V, Verges M, Larson M (2006) Experimental study and life prediction on high cycle vibration fatigue in BGA packages. Microelectron Reliab 46(7):1128–1138 (ISSN 0026–2714)
17. Qi H, Osterman M, Pecht M (2007) Plastic ball grid array solder joint reliability for avionics applications. IEEE Trans Compon Packag Technol 30(2):242–247
18. Samavatian M, Ilyashenko LK, Surendar A, Maseleno A, Samavatian V (2018) Effects of system design on fatigue life of solder joints in bga packages under vibration at random frequencies. J Electron Mater 47:6781–6790
19. Steinberg DS (1988) Vibration analysis for electronic equipment [M]. Wiley
20. Veprik AM (2003) Vibration protection of critical components of electronic equipment in harsh environmental conditions. J Sound Vib 259(1):161–175 (ISSN 0022–460X)
21. Wang H, Zhao M, Guo Q (2004) Vibration fatigue experiments of SMT solder joint. Microelectron Reliab 44(7):1143–1156 (ISSN 0026–2714)
22. Wong EH, Seah S, Shim V (2008) A review of board level solder joints for mobile applications[J]. Microelectron Reliab 48(11–12):1747–1758
23. Xie D, Zhang A, Kelly B, Lee J, Roucou R, Shi X, Doranga S, Khaldarov V, Hai J (2023) A New Vibration Test Method for Automotive and Consumer Electronic Devices: Calibration and Fatigue Test. IEEE 73rd Electron Compon Technol Conf (ECTC) Orlando, FL, USA 289–296
24. Yu D, Al-Yafawi A, Nguyen T, Park S, Chung S (2011) High-cycle fatigue life prediction for Pb-free BGA under random vibration loading. Microelectron Reliab 51(3):649–656 (ISSN 0026–2714)

Shifeng Yu is currently pursuing the master's degree with Central South University, Changsha, China.

Junjie Dai received the master's degree from Central South University, Changsha, China, in 2023.

Junhui Li was born in Taojiang, China, in 1969. He received Ph.D. degree in mechanical engineering from Central South University (CSU), Changsha, China, in 2008.He has been a professor with CSU, since September 2011. He is currently working on electronics packaging. He has published more than 80 papers. His research interests include electronics packaging and manufacturing.